IEEE Photonics Journal
An IEEE Photonics Society Publication

Open Access

Hybrid Ytterbium/Brillouin Gain Assisted Partial Mode Locking in Yb-Doped Fiber Laser

Volume 7, Number 3, June 2015

Haibin Lü
Pu Zhou
Xiaolin Wang
Zongfu Jiang

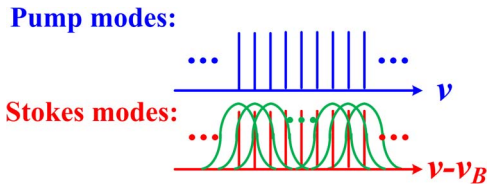

DOI: 10.1109/JPHOT.2015.2420620
1943-0655

IEEE photonics SOCIETY

IEEE

Hybrid Ytterbium/Brillouin Gain Assisted Partial Mode Locking in Yb-Doped Fiber Laser

Haibin Lü, Pu Zhou, Xiaolin Wang, and Zongfu Jiang

College of Optoelectric Science and Engineering, National University of Defense Technology, Changsha 410073, China

DOI: 10.1109/JPHOT.2015.2420620

Manuscript received January 28, 2015; revised March 28, 2015; accepted April 2, 2015. Date of publication April 6, 2015; date of current version April 24, 2015. This work was supported by the National Excellent Doctoral Dissertation of China (FANEDD), the Program for New Century Excellent Talents in University, and the Innovation Foundation for Graduates of the National University of Defense Technology. Corresponding author: P. Zhou (e-mail: zhoupu203@163.com).

Abstract: We have demonstrated experimentally and theoretically that the hybrid ytterbium/Brillouin gain can contribute to partial mode locking in the high-loss ytterbium-doped fiber laser. With only few cavity modes contained within the Brillouin gain curve, the dynamics of self-pulsing was not observed for the stimulated Brillouin scattering signal generated by each pump mode in the experiment. The results from two different experimental schemes show that both the Brillouin and ytterbium gains are required to support enough Brillouin pump and stokes cavity modes for partial mode locking. We also show that it is the coupling between the stimulated Brillouin scattering of the neighboring Brillouin pump modes that plays a direct role in the partial phase synchronization between different stokes modes. Furthermore, we proposed a theoretical model about the partially mode-locked laser dynamics. Based on the model, the numerical results agree quantitatively with the experimental ones. It is also found numerically that the extent of the phase synchronization can be enhanced by the cascaded stimulated Brillouin scattering according to the same physical mechanism.

Index Terms: Fiber laser, partial mode locking, stimulated Brillouin scattering.

1. Introduction

In recent years, much effort has been deployed to study various dynamic behaviors in fiber lasers, such as mode locking and Q-switching [1]–[4]. There are a lot of effective ways to realize them based on various nonlinear effects. Stimulated Brillouin scattering (SBS) is under intensive investigation for its responsibility for a large class of dynamic behaviors in different kinds of optical fiber systems, such as self-pulsing (or called "spontaneous mode locking") in cw-pumped single-mode long passive fiber cavities with a large number of cavity modes beneath the Brillouin gain curve [5]–[7], and passive Q-switching in much short ytterbium-doped fiber lasers [8]–[12]. For high-loss ytterbium-doped fiber lasers with conventional cavity configuration [10], [11], almost every single Q-switched intense pulse consists of a train of subpulses with interpulse time interval equal to the cavity round-trip time, which was attributed to the SBS dynamic instability in general terms. On the one hand, due that only few cavity modes are contained beneath the Brillouin linewidth in that case, no self-pulsing would happen for the SBS signal

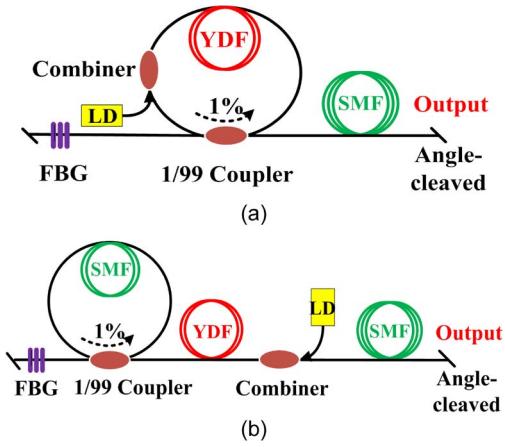

Fig. 1. Two different experimental setups. (a) Case 1. (b) Case 2. YDF: polarization-maintaining ytterbium-doped fiber; LD: laser diode; FBG: Fiber Bragg Grating; SMF: polarization-maintaining single-mode passive fiber.

generated by each one Brillouin pump mode [7]. On the other hand, the cavity modes of stokes light are supported by both the Brillouin and ytterbium gains in the ytterbium-doped fiber laser. Hence, influences of the hybrid ytterbium/Brillouin gains on the phase synchronization of the stokes modes should be considered, but to our knowledge, no detailed analysis of this phenomenon has been carried through up to now.

In this letter, we demonstrate experimentally and theoretically that hybrid ytterbium/Brillouin gain can support the partial mode locking in the high-loss ytterbium-doped fiber laser. The experimental results reveal that no self-pulsing is observed for the SBS signal generated by each pump mode, and that both the Brillouin and ytterbium gains are required to support enough Brillouin pump and stokes modes for the partial mode locking in the ytterbium-doped fiber laser. It is also presented experimentally that the direct mechanism for the partial phase synchronization between different stokes modes is the coupling between the SBS of the neighboring Brillouin pump modes due to the spectral overlap of Brillouin gain. Hence, such mode-locked instability is different from the self-pulsing dynamics observed for the SBS signal generated by each Brillouin pump mode. Furthermore, we propose a theoretical model about the hybrid ytterbium/Brillouin gain-based partially mode-locked laser dynamics. Based on the model, the numerical results agree well with the experimental ones, and present that the extent of the phase synchronization for the high-order stokes components can be enhanced by the cascaded SBS process according to the same mode-locked mechanism.

2. Experimental Setups

Two different experimental configurations of polarization-maintaining ytterbium-doped fiber laser systems are illustrated in Fig. 1. The main difference between the two cases is whether the single mode polarization-maintaining double-clad ytterbium-doped fiber (YDF) is placed within the ring cavity or not, while the other system parameters are kept the same. As shown in Fig. 1(b), the second scheme is designed to verify whether the dynamics of self-pulsing will occur for the SBS signal generated by each pump mode in the case that only Brillouin gain dominates in the ring cavity. The length of YDF in each configuration is around 10 m. Hence the total length of the ring cavity for each case is about 12 m with the mode spacing of approximately 15 MHz, indicating that there are about two or three ring-cavity modes within the Brillouin gain curve because the full bandwidth of the Brillouin gain spectrum is about 32 MHz at 1080 nm for the silica fiber (corresponding to the phonon lifetime of 5 ns) [13]. In order to excite the SBS, we employ the distributed Rayleigh feedback to narrow the laser linewidth [8]. The linewidth-narrowing is achieved with the linear cavity formed by a piece of polarization-maintaining single-mode

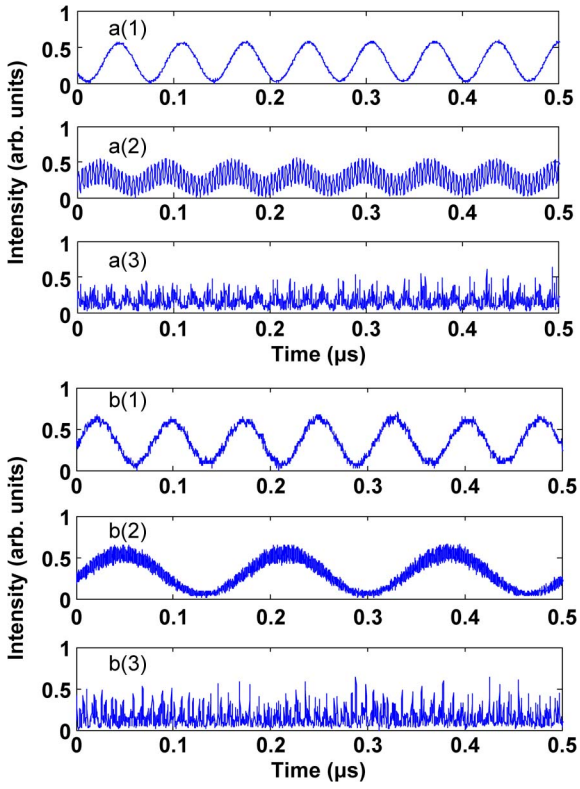

Fig. 2. Respective dynamics of the laser for the two different experimental cases when pump power P is below the corresponding SBS threshold. (a1)–(a2) P = 0.6 W; (a3) P = 0.8 W; (b1)–(b2) P = 0.9 W; (b3) P = 1.2 W.

passive fiber (SMF) and a polarization-maintaining Fiber Bragg Grating (FBG). The length of the SMF is about 500 m, and the output port of the SMF is angle-cleaved to suppress the end-face feedback. The FBG has a central wavelength of 1080 nm with the bandwidth of 0.2 nm, and its reflectivity is about 90%. The ring cavity is constructed by a polarization-maintaining 1/99 coupler with fast axis blocked. As studied in [11], the SBS-based Q-switched intense pulses cannot be observed in the low-loss laser cavity. Therefore, the feedback ratio for the light after one round trip inside the ring cavity is set to be about 1% for both two cases. A $(2+1)\times 1$ polarization-maintaining combiner is used to couple the 976-nm pump light into the system.

3. Experimental Results and Discussions

The laser thresholds for the two different experimental cases are around 0.5 W and 0.8 W, while the SBS thresholds for them are about 0.9 W and 1.5 W, respectively. For each case, when the pump power is below the corresponding SBS threshold, the laser dynamics is similar to the experimental results observed in [10], presenting as a train of irregularly sustained relaxation-oscillation pulses with the pulse width in the microsecond range. Fig. 2 shows the details of one single pulse at the different pump powers for the two schemes. For Case 1, when the pump power is just above the laser threshold, as presented in Fig. 2(a1) and (a2), the corresponding time evolution of the output intensity shows the time-dependent beating of different ring-cavity modes with the frequency of integral multiple of the mode spacing of the ring cavity, which is verified by calculating the corresponding power spectra. As a result of the distributed Rayleigh scattering in the system, the laser signals travel bidirectionally in the ring cavity. Thus, the spatial hole burning effect (SHB) is possible to occur in the ring cavity, as well as the self-induced laser line sweeping effect (SLLS) [14]. Through careful comparison between the power spectra

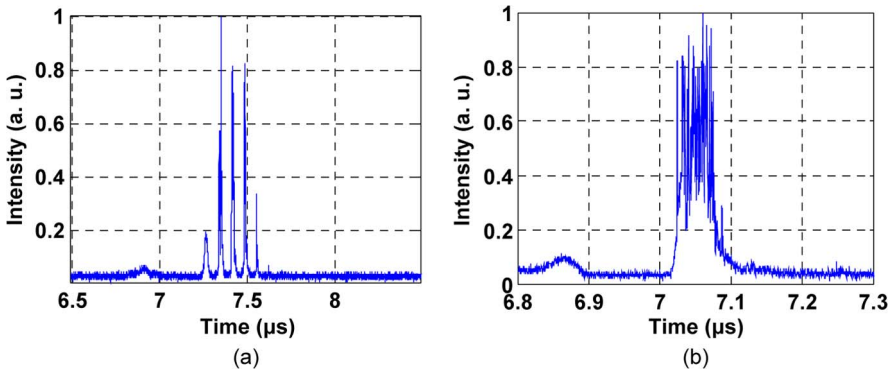

Fig. 3. Respective dynamics of the laser for each case when the pump power P is above the corresponding SBS threshold. (a) Case 1 (P = 1.2 W). (b) Case 2 (P = 1.7 W).

of different individual relaxation-oscillation pulses, it is found clearly that the composition of generated longitudinal modes is changed after switching from one pulse to another. Thus, according to the analysis in [15], it can be concluded that the SLLS effect, namely, the SHB effect, has occurred in our experiment. As the pump power increases further but is still below the corresponding SBS threshold, more and more Brillouin pump modes of the ring cavity start operating, and the corresponding output intensity presents clearly chaotic behaviors as shown in Fig. 2(a3). Similarly, it is also found that hopping to other different modes is confirmed for different single pulses in the pulse train by comparing the respective power spectra. Moreover, according to the theory proposed in [16], the SHB effect will lead to generation of equivalent dynamic gain and phase gratings in the active fiber. As a result, for a certain relaxation-oscillation pulse, the effective phase grating resulted from the gain-induced refractive index change caused by all the previous gain gratings will impose a time-dependent phase change on each longitudinal mode. Because the effective gain experienced by each mode is different, the phase change is also different from each other. Thus, when each pulse contains a large number of longitudinal modes at the quite high pump power, the details of the pulse can be thought of as the interference of the modes with random phase differences, and hence show clearly a transition to chaos. For Case 2, due that the YDF is outside of the ring cavity, the ring cavity does not play a significant role in the performance of the laser like in Case 1. Hence, the whole structure of cavity modes in the laser is constructed by not only the ring cavity but also a large number of equivalent linear cavities resulted from the randomly distributed Rayleigh feedback [17]. Therefore, details of the irregular pulses can be thought of as the interference of the modes supported by different cavities with arbitrary phases and amplitudes, as shown in Fig. 2(b1)–(b3).

When the pump power exceeds the corresponding SBS threshold for each case, the output intensity consists of a train of self-Q-switched intense pulses, but the details of every single Q-switched pulse are clearly different for Case 1 and 2, as shown in Fig. 3. For Case 1, every individual Q-switched intense pulse is made up of a sequence of subpulses with the pulse period equal to the round-trip time of the ring cavity, as observed in [10] and [11]. Resulted from the cascaded SBS process in the ytterbium-doped fiber laser, the Q-switched intense pulse is mainly comprised by the high-order stokes components [12]. Hence, occurrence of the structure of subpulses with pulse period equal to the round-trip time of the ring cavity suggests that a part of the stokes ring-cavity modes reach to the phase synchronization, which consequently gives rise to the partial mode locking. On the other hand, structure of mode-locked resembling subpulses is not observed for Case 2 in Fig. 3(b), and the stochastic fluctuations distributed on the shape of the Q-switched pulse may be attributed to the superimposition of the stokes cavity modes with arbitrary phases and amplitudes which are supported by the ring cavity and other different cavities resulted from the distributed Rayleigh feedback. Moreover, it also indicates that the SBS signal generated by each Brillouin pump ring-cavity mode presents no self-pulsing in the ring cavity. In fact, the ring-cavity mode spacing for both two cases is about 15 MHz so

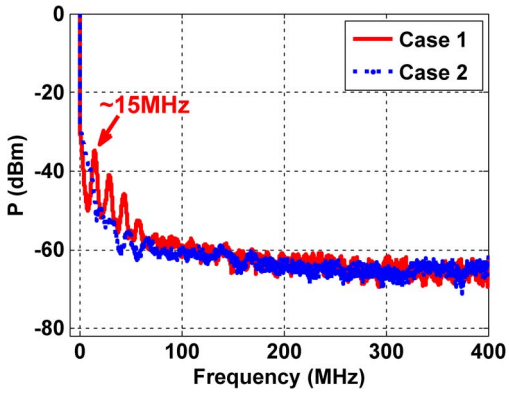

Fig. 4. Respective average power spectrums with the same pump powers as in Fig. 3 for both cases.

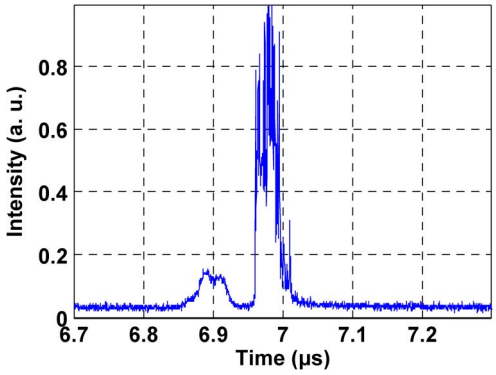

Fig. 5. Typical details of one single Q-switched intense pulse with the total ring-cavity length of 5 m at the pump power of 2.4 W.

that there are only two or three cavity modes contained beneath the Brillouin gain bandwidth. According to the theory about self-pulsing in the Brillouin fiber laser [7], no dynamics of self-pulsing can be observed for the SBS signal generated by each one pump mode. However, for Case 1, the stokes ring-cavity modes experience both Brillouin and ytterbium gains in the ring cavity so that the actual number of the ring-cavity modes of stokes light is much larger than that for Case 2, which is verified to a certain extent by the average power spectra for both two cases presented in Fig. 4. Therefore, because the mode spacing of Brillouin pump ring-cavity modes is less than the Brillouin gain bandwidth, the partial mode locking occurred in Case 1 may be considered as a result of the coupling between the SBS of the neighboring Brillouin pump ring-cavity modes due to the spectral overlap of the Brillouin gain. Furthermore, the influence of cascaded SBS process should also be taken into account and will be analyzed carefully in the theoretical model.

In order to prove that it is the coupling between the SBS of the neighboring Brillouin pump modes that pulls the different ring-cavity modes of the stokes components to reach to the partial phase synchronization, the experiment with the first scheme (see Case 1) is repeated but the total length of the ring cavity is reduced to 5 m, which means that the mode spacing is about 40 MHz and larger than the Brillouin bandwidth. The laser threshold occurs at the pump power of 1.3 W, and the SBS threshold is about 2.2 W. When the pump power is below the SBS threshold, the dynamics of the fiber laser is similar to that for Case 1, presenting as the beating of the Brillouin pump ring-cavity modes and chaos at the different pump powers. As the pump power increases above the SBS threshold, the output intensity likewise consists of a train of Q-switched gigantic pulses. However, as shown in Fig. 5, the details of every individual Q-switched pulse

present no mode-locked resembling subpulses with the inter-pulse interval equal to the ring-cavity round-trip time, which is absolutely distinct from that for Case 1. In addition, a relatively low intensity peak occurs in advance of the principal Q-switched intense pulse with around 100 ns, as well as for Case 1 and 2, which is usually considered as the prelasing signature [8].

Comparison between the experimental results presented in Figs. 3(a) and 5 tells us that no partial mode locking happens when the mode spacing of the ring cavity is larger than the Brillouin bandwidth. With the experimental results in Fig. 3(b) taken into account additionally, it appears to suggest that, as a result of the spectral overlap of the Brillouin gain, the coupling between the SBS of the neighboring Brillouin pump modes is the direct mechanism responsible for the partial phase synchronization between the cavity modes of the stokes components in the experiment.

Therefore, for an Yb-doped fiber laser with the total length of the cavity short enough to make sure that no self-pulsing would happen for the SBS signal generated by each Brillouin pump mode, we believe that the qualitative process of the partial mode locking observed in the experiment can be elucidated by the following model with the influence of cascaded SBS process taken into account. First, with the pump power increasing above the laser threshold but still below the SBS threshold, there is an increasing number of Brillouin pump modes, amplified by the ytterbium gain, oscillating in the laser cavity. When the pump power increases above the SBS threshold, the most powerful pump mode excites the SBS noise firstly, and then the seed of the first-order stokes component is amplified by both the Brillouin and ytterbium gains, resulting in that the real number of stokes cavity modes oscillating is much larger than that supported by only the Brillouin gain. With the mode spacing of the stokes cavity modes less than the Brillouin gain bandwidth, each pump mode can exchange power with several adjacent stokes cavity modes which are located beneath the Brillouin gain curve. Moreover, because the mode spacing of the Brillouin pump modes is approximately equal to that of the stokes modes in the laser cavity, there exists spectral overlap of the Brillouin gain between the neighboring Brillouin pump modes. As a result, different cavity modes of the first-order stokes component are correlated by the coupling between the SBS of the neighboring Brillouin pump modes and pulled to reach to the phase synchronization in part. In the same way, for the second-order stokes component, the amplified first-order stokes component plays the role of Brillouin pumping and pulls the cavity modes of the second-order stokes component to be more correlative by the coupling between the SBS of its neighboring cavity modes. Similarly, the mentioned-above mode-locked mechanism also applies to the higher-order stokes components, which eventually gives rise to the partial mode locking observed in the experiment. As a whole, both the ytterbium and Brillouin gains are required to realize the partial mode locking in the ytterbium-doped fiber laser with relatively short cavity configuration.

On the other hand, as discussed above, the SHB effect occurs in the experiment. Thus, it is necessary to analyze the influence of the SHB effect on the partial mode locking process observed in our case. According to the theory proposed in [15] and [16], the lifetime of dynamic gratings is determined by the lifetime of the upper level of the laser transition and is about 0.8 ms for Yb-doped fiber lasers. Moreover, it should be noted that it is the gain grating that selects different composition of longitudinal modes for different relaxation-oscillation pulses, namely determining the generation of the next pulses. Meanwhile, the phase grating will impose a linear frequency chirp within each pulse. Due to the high enough peak power and narrow width of the instantaneous laser spectrum, SBS is observed with increasing the pump power. As a result, the laser dynamics presents a clear transition from relaxation oscillation to self-Q-switched gigantic pulses which are mainly comprised by the high-order stokes components. The average pulse duration of each Q-switched pulse is about 200 ns, which is much less than that of the relaxation oscillation pulse (about 10 μs). Therefore, it is reasonable to consider the effective gain and resultant phase gratings to be stationary during the whole duration of each Q-switched pulse. Thus, the partial mode locking process observed within each Q-switched pulse is mainly defined by the coupling between the SBS of the neighboring Brillouin pump ring-cavity modes due to the spectral overlap of the Brillouin gain and cascaded SBS process. Furthermore, the excited

acoustic wave during the SBS process decays rapidly with a lifetime of about 5 ns in silica-based optical fiber, which is much less than the average period of Q-switched pulses (about 200 μs). Thus, it indicates that the SBS of the adjacent Q-switched pulses is totally independent, which is clearly different with the process of the dynamic gratings. As a whole, we can conclude that the dynamic gratings induced by the SHB effect impose little influence on the partial mode locking process observed in our experiment.

4. Theoretical Model and Numerical Results

In order to verify the aforementioned qualitative deductions, we propose a theoretical model about the hybrid ytterbium/Brillouin gain-based partially mode-locked laser dynamics in an ytterbium-doped fiber ring laser. In our model, the dynamic mechanisms considered mainly include the population inversion, laser amplification, cascaded SBS process, spontaneous emission noise, and SBS noise. Furthermore, because the stokes components originate mainly from the SBS of the laser signal, hence we assume that only the laser signal comes from the spontaneous emission noise. Besides, the YDF in the ring cavity is much longer than the passive fiber (the pigtails of the coupler and pump combiner); hence, we assume that it is reasonable to neglect the difference between the SBS frequency shifts in the ytterbium-doped and passive fibers. Total three orders of the SBS process are considered in the model, and the final set of temporal-spatial equations describing the laser dynamics are given by [12], [13], [18]

$$\begin{aligned}
\pm\frac{\partial A_k^{\pm}}{\partial z}+\frac{1}{v_g}\frac{\partial A_k^{\pm}}{\partial t} &= \frac{1}{2}\left(g_k^{\pm}-\alpha_s\right)A_k^{\pm}+i\kappa_1\left(A_{k-1}^{\mp}\left(Q_k^{\mp}\right)^{*}+A_{k+1}^{\mp}Q_{k+1}^{\pm}\right)+\eta_k f_{SE}^{\pm}(z,t)\\
\frac{\partial Q_k^{\pm}}{\partial t} &= -\frac{\Gamma_B}{2}Q_k^{\pm}+i\kappa_2 A_{k-1}^{\pm}\left(A_k^{\mp}\right)^{*}+f_k^{\pm}(z,t)\\
\pm\frac{\partial P_p^{\pm}}{\partial z}+\frac{1}{v_p}\frac{\partial P_p^{\pm}}{\partial t} &= -\alpha_p P_p^{\pm}-\Gamma_p\left\{\sigma_{ap}N_1-\sigma_{ep}N_2\right\}P_p^{\pm}\\
\frac{\partial N_2}{\partial t} &= -\frac{N_2}{\tau}+\frac{\Gamma_p\lambda_p}{hcA}\left\{\sigma_{ap}N_0-(\sigma_{ap}+\sigma_{ep})N_2\right\}\left(P_p^{+}+P_p^{-}\right)\\
&\quad+\frac{\Gamma_s}{hcA}\sum_k\lambda_k\left\{\sigma_{ak}N_0-(\sigma_{ak}+\sigma_{ek})N_2\right\}\left(\left|A_k^{+}\right|^2+\left|A_k^{-}\right|^2\right)
\end{aligned}$$

where $g_k=(\sigma_{ek}+\sigma_{ak})N_2-\sigma_{ak}N_0$. α_s and α_p is the absorption coefficients of the YDF at the laser and pump wavelengths; c is the velocity of light in vacuum; ν_g and ν_p are the group velocities of the laser and pump light; κ_1 and κ_2 are the coupling coefficients of the SBS process [13]; Γ_B is the acoustic damping rate; $\{\sigma_{ap},\sigma_{ep}\}$ and $\{\sigma_{ak},\sigma_{ek}\}$ are the absorption and emission cross sections at the pump (λ_p) and laser (λ_k) wavelengths; A is the doped cross-section area; Γ_p (Γ_s) is the overlapping factor between the pump (laser) and the fiber doped area; N_0 is the ytterbium dopant concentration and assumed to be uniform along the YDF, and N_2 is upper-level population; τ is the upper-level lifetime. $P_p(z,t)$ is the pump power; $\{A_k(z,t),\ k=0,1,2,3\}$ are the complex amplitudes of the light waves at the lasing $(k=0)$ and at the three-order SBS-shifted ($k=1,2,3$) frequencies, and are normalized to make $P_k=|A_k|^2$, where P_k are the corresponding powers; $\{Q_k(z,t),\ k=1,2,3\}$ are the complex amplitudes of the acoustic waves corresponding to the three-order cascaded SBS processes. The superscript "+" denotes the anticlockwise propagation and "−" denotes clockwise propagation, respectively. η_k is set to be 1 only when k equals to 0, otherwise, η_k is set to be 0. The spontaneous emission noise $f_{SE}^{\pm}(z,t)$ and Langevin noise sources $\{f_k^{\pm}(z,t)\}$ are both Gaussian stochastic processes with zero mean and, therefore, satisfy [18], [19]

$$\begin{aligned}
\left\langle f_{SE}^{\pm}(z,t)f_{SE}^{\pm^*}(z',t')\right\rangle &= \Lambda_{SE}\delta(z-z')\delta(t-t')\\
\left\langle f_k^{\pm}(z,t)f_k^{\pm^*}(z',t')\right\rangle &= N_{ac}\delta(z-z')\delta(t-t')
\end{aligned}$$

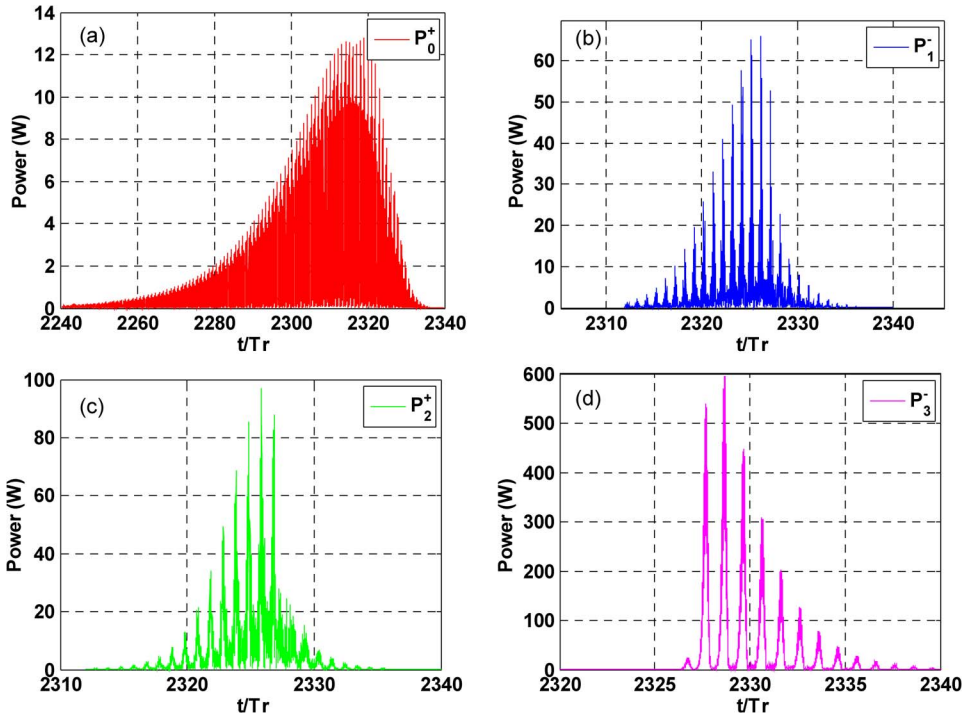

Fig. 6. Typical simulated results for the output powers. (a) P_0^+; (b) P_1^-; (c) P_2^+; (d) P_3^-. T_r is the round-trip time of the ring cavity. The simulation parameters are as follows: the total cavity length is 12 m; the YDF length is 10 m; the ring-cavity feedback ratio is 1%; $P_p = 1.2$ W, $\lambda_p = 976$ nm, $N_0 = 6.4 \times 10^{24}$ m^{-3}, $\tau = 840$ μs, $\Gamma_p = 0.01$, $\Gamma_s = 0.85$, $A = 30$ μm^2, $A_{eff} = 46$ μm^2, $\Gamma_B/2\pi = 32$ MHz, $g_B = 4\kappa_1\kappa_2 A_{eff}/\Gamma_B = 2.54\times10^{-11}$ m/W, $v_A = 5.96$ km/s, $\sigma_{ap} = 4.37\times10^{-24}$ m^2, $\sigma_{ep} = 4.41\times10^{-24}$ m^2, $\sigma_{as} = 5.0 \times 10^{-27}$ m^2, $\sigma_{es} = 3.3 \times 10^{-25}$ m^2, $\alpha_p = 0.002$, and $\alpha_s = 0.003$.

where $\Lambda_{SE} = 2\sigma_{ek}N_2(z,t)hc^2\Delta\lambda/\lambda_0^3$, and $N_{ac} = 2k_BT\rho_0\Gamma_B/v_A^2A_{eff}$. $\Delta\lambda$ is the bandwidth of the laser signal; k_B is the Boltzmann constant; T is the environmental temperature; ρ_0 is the average material density; v_A is the velocity of the acoustic wave in fiber; and A_{eff} is the acousto-optic effective area.

Based on the theoretical model mentioned above, we simulated numerically the partially mode-locked dynamics in an Yb-doped fiber ring laser with the simulation parameters corresponding to the experimental conditions in Case 1. The detailed simulation conditions are as follows: the pump scheme is likewise single-end pumping according to that in Case 1, which corresponds that we assume that only P_p^- is taken into account (of course, we can also assume that only P_p^+ is considered); the simulation parameters of the YDF match entirely with the real fiber parameters of the YDF employed in Case 1; the total cavity length and the feedback ratio in the simulation are also the same with those in Case 1. The simulation results under the aforementioned conditions are shown in Fig. 6. It should be clarified that, because there are two counter-propagation groups of laser-stokes components, i.e., $\{A_0^+, A_1^-, A_2^+, A_3^-\}$ and $\{A_0^-, A_1^+, A_2^-, A_3^+\}$, in the ring cavity and the dynamics for them are similar, we only show the dynamics of the first group for simplicity.

As shown in Fig. 6, we can see clearly that the SBS-based Q-switched pulse is mainly comprised by the high-order stokes components. More importantly, comparison among the simulated results presented in Fig. 6(a)–(d) suggests that, the detailed pulse shape of the Q-switched laser pulse [see Fig. 6(a)] is made up of the superimposition of the laser modes with arbitrary phases, similar with the experimental details shown in Fig. 2(a3), and consequently presents no mode-locked resembling subpulses with the pulse period equal to the round-trip time of the ring cavity. However, occurrence of the structure of mode-locked resembling subpulses is evident for the

SBS stokes components. Especially for the third-order stokes component, the simulated result in Fig. 6(d) quantitatively reproduces the temporal structure of the Q-switched pulse presented in Fig. 3(a) for Case 1. Therefore, when the mode spacing of the laser cavity is less than the Brillouin gain bandwidth, the coupling between the SBS of the neighboring Brillouin pump modes due to the spectral overlap of the Brillouin gain can pull the different cavity modes of the stokes components to reach to the partial phase synchronization and the extent of synchronization can be enhanced by the cascaded SBS process, which is verified clearly by the simulated results presented in Fig. 6(b)–(d).

Furthermore, In order to prove that there are no self-pulsing for the SBS signal generated by each Brillouin pump mode in the ring cavity for both Case 1 and Case 2, we study the SBS dynamics of the Brillouin ring laser with the conditions employed in the experiment. As a result, the total cavity length L is 12 m, and the feedback for the Stokes field after one round-trip inside the ring cavity $R = 0.01$. As presented in [7], a linear stability analysis of the SBS coupled equations predicts that the CW state of the ring laser is unstable whenever the small-signal gain G satisfies $G_1 < G < G_2$, where $G_1 = \ln(1/R)$ and $G_2 = \ln((1 + 2R)/3R)$. The laser threshold is reached when $G = G_1$. However, this inequality is generally available for the case that the length L of the ring cavity is large enough to permit a large number of longitudinal modes N beneath the Brillouin gain curve. If $N \sim 1$, the dynamics can be only stationary. For the case in our experiment, N is calculated to be about 2 ($L[\mathrm{m}]/5\lambda^2[\mu\mathrm{m}]$, where λ is the pump wavelength). In order to verify whether the aforementioned inequality applies to our case, we numerically solved the SBS coupled equations with the corresponding boundary conditions. The numerical results suggest that the stokes field eventually evolves to the CW state even when the gain G satisfies $G_1 < G < G_2$. Moreover, numerical simulations are also performed for the case when $G > G_2$. Similarly, the stokes eventually tends to the CW state and presents no self-pulsed dynamics. Therefore, we can conclude that, for the case in our experiment, there is no self-pulsing for the SBS signal generated by each Brillouin pump ring-cavity mode.

At last, in order to verify numerically the experimental results presented in Fig. 5, Fig. 7 shows the simulated results when the total cavity length is reduced to 5 m with the YDF length of 4 m, which means that the mode spacing of the ring cavity increases to be about 40 MHz and is larger than the Brillouin gain bandwidth. The other simulation parameters keep the same with those used in Fig. 6.

As shown in Fig. 7, the SBS-based Q-switched pulse is also mainly comprised by the high-order stokes components when the cavity length is reduced to 5 m. Moreover, the output temporal characteristics of the third-order stokes component agrees qualitatively with the Q-switched pulse depicted in Fig. 5, and is attributed to the superimposition of the stokes ring-cavity modes with arbitrary phases. Furthermore, comparison between the simulated results given in Figs. 6 and 7 suggests clearly that the extent of the phase synchronization between the cavity modes for all the stokes components decreases when the mode spacing exceeds the Brillouin gain bandwidth. It indicates that the extent of the coupling between the SBS of the neighboring Brillouin pump modes decreases due to the increasing mode spacing of the laser cavity.

Moreover, as studied in [11], the cavity loss imposes an important influence on the dynamics of the laser. When the laser cavity is a low-loss cavity, there is no occurrence of the SBS-based Q-switched dynamics, which can be also verified by our model. It is found by our numerical results that the intensity of the highest-order stokes component dominates in the cavity with respect to the laser and the other stokes components and tends to the quasi-CW state, which is characterized by the fast oscillation resulted from the longitudinal mode beating with arbitrary phases, rapidly through the relaxation oscillation process [20]. Due that a low-loss cavity leads to the more uniform intra-cavity intensity distribution and longer cavity lifetime of the photons than the high-loss cavity [21], the laser and the stokes components evolve to the quasi-CW state rapidly so that the sustained SBS-based Q-switching process cannot build up. Moreover, under the quasi-CW state, intensities of the laser and stokes components are not large enough to generate strong Brillouin gain for the next-order stokes component, and the ytterbium gain

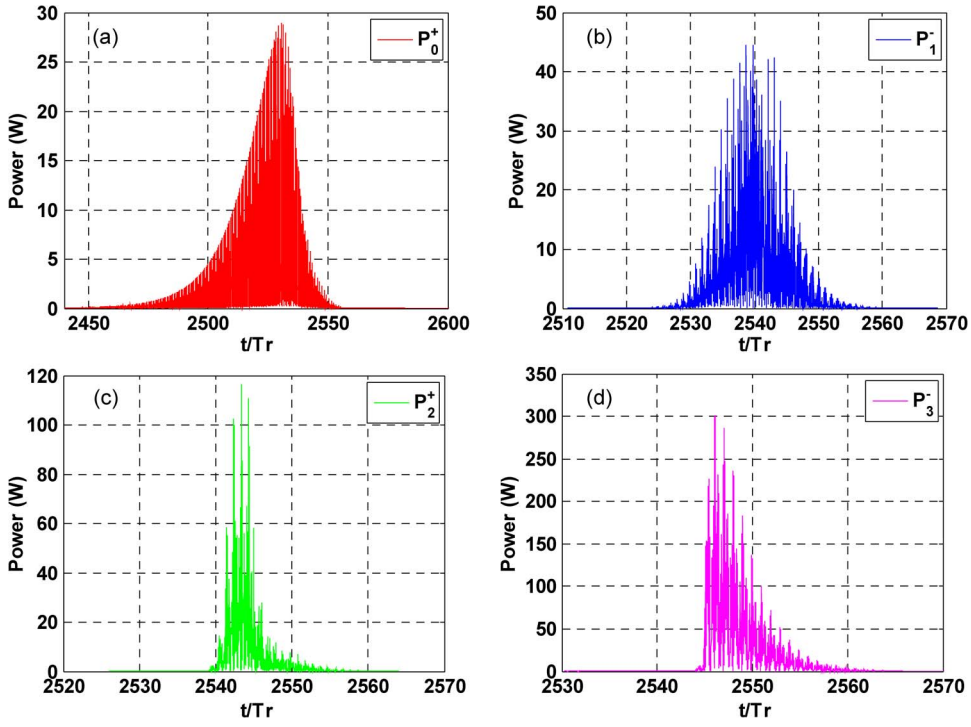

Fig. 7. Typical simulated results for the output powers. (a) P_0^+; (b) P_1^-; (c) P_2^+; (d) P_3^-. The total cavity length is reduced to 5 m with the YDF length of 4 m, and the pump power is 2.4 W. The other simulation parameters keep the same with those used in Fig. 6.

therefore dominates the dynamics in the cavity. As a result, there is no partial mode locking observed in the temporal output of the stokes components.

5. Conclusion

In conclusion, we demonstrate experimentally and theoretically that hybrid ytterbium/Brillouin gain can support the partial mode locking in a high-loss ytterbium-doped fiber laser with the mode spacing less than the Brillouin gain bandwidth. We show that both the ytterbium and Brillouin gains are required to support enough Brillouin pump and stokes cavity modes in the ytterbium-doped fiber laser. Moreover, further experimental and numerical results indicate that it is the coupling between the SBS of the neighboring Brillouin pump modes that pulls the stokes modes to reach to the partial phase synchronization and the extent of the phase synchronization for the high-order stokes components can be enhanced by the cascaded SBS process according to the same mode-locked mechanism, which eventually give rise to the partial mode locking observed in the ytterbium-doped fiber laser with relatively short cavity configuration.

References

[1] J. Chen, J. W. Sickler, E. P. Ippen, and F. X. Kärtner, "High repetition rate, low jitter, low intensity noise, fundamentally mode-locked 167 fs soliton Er-fiber laser," *Opt. Lett.*, vol. 32, no. 11, pp. 1566–1568, Jun. 2007.
[2] L. Zhang *et al.,* "Linearly polarized 1180-nm Raman fiber laser mode locked by graphene," *IEEE Photon. J.*, vol. 4, no. 5, pp. 1809–1815, Oct. 2012.
[3] Y. Zhao and S. D. Jackson, "Passively Q-switched fiber laser that uses saturable Raman gain," *Opt. Lett.*, vol. 31, no. 6, pp. 751–753, Mar. 2006.
[4] J. Liu, S. Wu, Q.-H. Yang, and P. Wang, "Stable nanosecond pulse generation from a graphene-based passively Q-switched Yb-doped fiber laser," *Opt. Lett.*, vol. 36, no. 20, pp. 4008–4011, Oct. 2011.
[5] I. Bar-Joseph *et al.,* "Spontaneous mode locking of single and multi-mode pumped SBS fiber lasers," *Opt. Commun.*, vol. 59, no. 4, pp. 296–298, Sep. 1986.

[6] V. Lecoeuche, B. Ségard, and J. Zemmouri, "Modes of destabilization of Brillouin fiber ring lasers," *Opt. Commun.*, vol. 134, no. 1–6, pp. 547–558, Jan. 1997.
[7] C. Montes *et al.,* "Self-pulsing and dynamic bistability in cw-pumped Brillouin fiber ring lasers," *J. Opt. Soc. Amer. B, Opt. Phys.*, vol. 16, no. 6, pp. 932–951, Jun. 1999.
[8] S. V. Chernikov, Y. Zhu, and J. R. Taylor, "Supercontinuum self-Q-switched ytterbium fiber laser," *Opt. Lett.*, vol. 22, no. 5, pp. 298–300, Mar. 1997.
[9] Z. J. Chen, A. B. Grudinin, J. Porta, and J. D. Minelly, "Enhanced Q switching in double-clad fiber lasers," *Opt. Lett.*, vol. 23, no. 6, pp. 454–456, Mar. 1998.
[10] M. Salhi *et al.,* "Evidence of Brillouin scattering in an ytterbium-doped double-clad fiber laser," *Opt. Lett.*, vol. 27, no. 15, pp. 1294–1296, Aug. 2002.
[11] B. Ortaç *et al.,* "Influence of cavity losses on stimulated Brillouin scattering in a self-pulsing side-pumped ytterbium-doped double-clad fiber laser," *Opt. Commun.*, vol. 259, no. 4–6, pp. 236–241, Jan. 2003.
[12] A. A. Fotiadi, P. Mégret, and M. Blondel, "Dynamics of a self-Q-switched fiber laser with a Rayleigh-stimulated Brillouin scattering ring mirror," *Opt. Lett.*, vol. 29, no. 10, pp. 1078–1080, May 2004.
[13] G. P. Agawal, *Nonlinear Fiber Optics*. San Diego, CA, USA: Academic, 1995.
[14] P. Peterka *et al.,* "Self-induced laser line sweeping in double-clad Yb-doped fiber-ring lasers," *Laser Phys. Lett.*, vol. 9, no. 6, pp. 445–450, Jun. 2012.
[15] I. A. Lobach, S. I. Kablukov, E. V. Podivilov, and S. A. Babin, "Broad-range self-sweeping of a narrow-line self-pulsing Yb-doped fiber laser," *Opt. Exp.*, vol. 19, no. 18, pp. 17632–17649, Aug. 2011.
[16] I. A. Lobach, S. I. Kablukov, E. V. Podivilov, and S. A. Babin, "Self-scanned single-frequency operation of a fiber laser driven by a self-induced phase grating," *Las. Phys. Lett.*, vol. 11, no. 4, Apr. 2014, Art. ID. 045103.
[17] S. K. Turitsyn *et al.,* "Random distributed feedback fibre laser," *Nat. Photon.*, vol. 4, pp. 231–235, 2010.
[18] Y. Wang and H. Po, "Dynamic characteristics of double-clad fiber amplifiers for high-power pulse amplification," *J. Lightw. Technol.*, vol. 21, no. 10, pp. 2262–2270, Oct. 2003.
[19] R. W. Boyd, K. Rzyzewski, and P. Narum, "Noise initiation of stimulated Brillouin scattering," *Phys. Rev. A*, vol. 42, no. 9, pp. 5514–5521, Nov. 1990.
[20] A. E. Siegman, *Lasers*. Mill Valley, CA, USA: Univ. Sci., 1986.
[21] A. Hideur, T. Chartier, C. Ozkul, and F. Sanchez, "Dynamics and stabilization of a high power side-pumped Yb-doped double-clad fiber laser," *Opt. Commun.*, vol. 186, no. 4–6, pp. 311–317, Dec. 2000.